Amplification and phase conjugation of weak signals

O. V. Kulagin, G. A. Pasmanik, A. A. Shilov

Institute of Applied Physics, Russian Academy of Sciences, Nizhniĭ Novgorod

(Submitted 3 December 1991; resubmitted after revision 29 January 1992)
Usp. Fiz. Nauk **162**, 129–157 (June 1992)

The results of the study on phase conjugation of weak optical signals with an energy of several photons are considered. Basic concepts of a semi-classical theoretical approach to describe amplification and phase conjugation (PC) of such signals are presented. A review is given of the experimental investigations that allowed reaching a limiting (about 1 photon per mode) sensitivity of optical systems with PC-mirrors for a large ($\sim 10^5$) number of resolution elements. High-sensitivity PC-mirror optical systems are demonstrated for a variety of applications.

1. INTRODUCTION

The problem of phase conjugation (PC) of extremely weak signals with an energy of several photons arises in the study of diverse optical systems, primarily those involving optical or brightness amplifiers. These systems are used in physical and other experiments, generally when it is necessary to record radiation by its coherent properties. Among such applications, in particular, is recording of holograms and interferograms of light reflected from the ground, a water surface, etc., and diffusely scattered over large areas. Optical amplifiers commonly induce aberrations in the light waves passing through them, which can be corrected by PC-mirrors.

Let us consider a simplified optical scheme (Fig. 1) that consists of a light source *1* illuminating a scattering object *2*, an input lens *3* followed by a brightness amplifier *4*, and a matrix photodetector *5*. For the illumination source we use a laser that sends to the object a light pulse with a time-constant transverse structure; it is a pulse of coherent UV, visible or IR radiation. We now assume that the pulsed radiation with the energy density ω is scattered diffusely and uniformly within an angle of 2π.

For simplicity the object plane is assumed to be perpendicular to the optical system axis. Let us choose some spot with an area ΔS on the object surface. The scattered light field in this area can be expanded in different sets of orthogonal functions; each of them is recalculated using the wave equation for the plane of the lens placed at a distance L from the object. Let us consider such a set in which the functions after recalculation remain orthogonal also on the lens surface of an area S_0. (It was shown in Ref. 1 that this is the only set of modes, which is found by solution of the corresponding integral equation which depends on the apertures of emitter and receiver, i.e., on the chosen area on the object and the lens surface.) The corresponding field components are attenuated after recalculation for the lens surface area of a limited aperture. One can distinguish a characteristic number of components ΔQ whose power is reduced to no more than half the power of the most intensive mode. They are the components that form, in the main, the field of the input signal on the optical system lens surface. The characteristic energy per component in an optical losses-free medium is equal to the value[1)]

$$\Delta W/\Delta Q = (w\Delta S/\Delta Q)\Omega/2\pi, \tag{1}$$

where $\Omega = S_0/2\pi$ is the solid angle in which the pulsed radiation scattered by the object can be recorded. To estimate ΔQ we assume the area ΔS and the lens aperture to be circular, with diameters D and D_0, respectively ($\Delta S = \pi D^2/4$; $S_0 = \pi D_0^2/4$).

In the considered case of circular apertures and uniform medium between the object and the lens the number

$$\Delta Q = (kDD_0/4L)^2 \tag{2}$$

is equal to the square of the so-called Fresnel number that characterizes the transmission capacity of two diaphragms with diameters D and D_0, spaced at a distance L ($k = 2\pi/\lambda$, λ is the wavelength). By substitution of (2) into (1) we have

$$\Delta W/\Delta Q = w\lambda^2/8\pi. \tag{3}$$

It is quite obvious that the number of resolution elements on the object surface area ΔS coincides with the number of orthogonal components forming the input field on the lens surface area with diameter D_0. Therefore, formula (3) can also be obtained in a different way. To this end it is enough to find the energy of the input signal arriving at the lens from one resolution element in the object plane. The lens angular resolution limited by diffraction is of the order of $(4/kD_0)$, which corresponds to a resolution element of size $d = (4/kD_0)L$ on the object surface. The energy emitted by the object surface area of diameter d is equal to $(\pi d^2/4)\cdot\omega$. Since only a part of this energy ($\sim\Omega/2\pi$) reaches the lens, we can find that the energy of radiation entering the optical

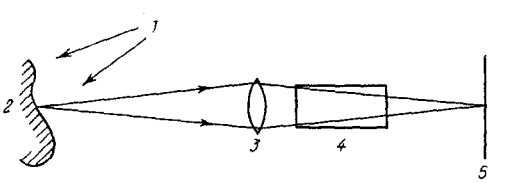

FIG. 1. *1*—an illuminating laser beam; *2*—scattering object; *3*—lens; *4*—brightness amplifier; *5*—matrix photodetector.

 0038-5670/92/060506-14$03.00

system from one resolution element is $(\pi d^2/4)\omega(\Omega/2\pi)$. By substituting the values of d and Ω we find formula (3).

From general considerations it is clear that the energy per one resolution element must be higher than 1 photon. Therefore, the minimal energy density on the illuminated object surface must satisfy the relation

$$w > w_{\min} = 8\pi\hbar\omega/\lambda^2. \tag{4}$$

The value of $\omega_{\min} \sim 1/\lambda^3$, which accounts, in particular, for a higher (than in the optical region) sensitivity of radio methods of spatial characteristics measurements for distant radiation sources such as, for example, stars, using super-long baseline interferometers.

2. SEMI-CLASSICAL APPROACH

In ordinary systems the information signal with the energy from a resolution element determined by formula (3) is recorded directly by a matrix photodetector placed either in the image or some other plane. However, there are other detection techniques that use coherent properties of a signal.

Here we mean recording of an interference pattern formed by the incoming signal and an auxiliary reference wave (heterodyning methods), as well as recording of the information signal pre-amplified in a quantum or any other optical amplifier (methods involving brightness amplifiers).

Let us consider methods of information signal recording from the point of view of reaching limiting sensitivity restricted by quantum noise. First of all, one needs to formulate an approach to describe the interaction of low-energy pulsed light fields with matter and with other fields of higher power.

We believe the so-called semi-classical approximation to be the most convenient one for this purpose. A light field within this approach is regarded as an ordinary classical wave $\mathscr{E}$ to which on entering a nonlinear medium a noise field $\mathscr{E}_N$ of vacuum zero-point fluctuations is added, whose correlation function for a given ambient temperature T is described by an ordinary (classical) Källen–Welton relation. However, to determine the correlation function of a light field of any order of magnitude at the optical system output so that the result would be in agreement with experiment, one needs to subtract from the calculated value for the correlation function of the total field the corresponding correlation function of zero-point fluctuations. For example, for intensity and its variance we have:

$$\begin{aligned} \langle I\rangle &= \langle I'\rangle - \langle I'_N\rangle, \\ \langle(\Delta I)^2\rangle &= \langle(\Delta I')^2\rangle - \langle(\Delta I'_N)^2\rangle; \end{aligned} \tag{5}$$

Here $I' = (c/2\pi)\cdot|\hat{K}(\mathscr{E} + \mathscr{E}_N)|^2$ is the ordinary classical intensity of a light wave with a complex amplitude defined as a sum of the input field $\mathscr{E}$ and the noise field $\mathscr{E}_N$ of vacuum zero-point fluctuations, $I'_N = (c/2\pi)|\mathscr{E}_N|^2$ is the zero-point fluctuations intensity, $\hat{K}$ is the operator that describes the brightness amplifier properties and its internal noise. For $\hat{K} = 1$ formulae (5) describe the process of radiation recording with an ordinary matrix photodetector.

It is impossible to substantiate consistently formulae (5) within the framework of classical electrodynamics. We can, though, make use of the values calculated earlier for some physical processes listed in Table I for the quantities measured in the experiment (mean photon number $\langle n\rangle$, and in some instances also the variance $\langle(\Delta n)^2\rangle$). The results obtained by traditional methods coincide with those yielded by the semiclassical approach considered here.

In all the experiments discussed below we report recording of the energy density distribution rather than the intensity distribution in a pulsed light beam that had passed through a brightness amplifier, and provide only a qualitative analysis of the time oscillations of radiation, while the oscillations themselves are measured only at certain points of a cross-section. Therefore, to compare theory and experiment it is convenient to integrate I' over time and by analogy with (5) to determine the values of the experimentally recorded energy density $\langle w\rangle$ and variance $\langle(\Delta w)^2\rangle$:

$$\begin{aligned} \langle w\rangle &= \langle w'\rangle - \langle w'_N\rangle, \\ \langle(\Delta w)^2\rangle &= \langle(\Delta w')^2\rangle - \langle(\Delta w'_N)^2\rangle, \end{aligned} \tag{6}$$

where $w' = \int_{-\infty}^{+\infty} I'\,dt$ is the classical energy density of a light wave with the complex amplitude $\mathscr{E} + \mathscr{E}_N$, $w'_N = \int_{-\infty}^{+\infty} I'_N\,dt$ is the energy density of zero-point fluctuations. One should bear in mind, that the variance of the above time-averaged values provides information only on radiation oscillations over a cross-section.

We define the photon numbers related to the intensity I' as

$$n' = \frac{\int_{-\infty}^{+\infty}\int_{\Delta S'} I'\,dt\,dS}{\hbar\omega\Delta Q'} = \frac{1}{\hbar\omega}\frac{\Delta W'}{\Delta Q'}, \tag{7}$$

TABLE I.

Type of physical process	Amplification (attenuation) coefficients range
1. Amplification in a quantum amplifier	$K \gg 1$
2. Amplification by stimulated scattering and four-wave mixing	
3. Spontaneous radiation	
4. Spontaneous scattering	$K - 1 \ll 1$
5. Direct registration of signals by a photodetector	$K = 1$
6. Thermodynamic equilibrium	
7. Black body radiation	$K \ll 1$

where $\hbar\omega$ is the quantum energy,

$$\Delta W' = \int_{-\infty}^{+\infty} \int_{\Delta S'} I' \mathrm{d}t\, \mathrm{d}S$$

is the classical value of the energy of radiation passing through an optical system in the cross-section area $\Delta S'$ with $\Delta Q'$ resolution elements, $\Delta W'/\Delta S'$ is the energy of radiation per resolution element in the optical cross-section (the number of resolution elements here is chosen irrespectively of the energy $\Delta W'$).

By analogy with (5) and (6) we find the mean photon number $\langle n \rangle$ and the variance $\langle (\Delta n)^2 \rangle$ recorded in the experiment, using the formulae

$$\begin{aligned} \langle n \rangle &= \langle n' \rangle - \langle n'_{\mathrm{N}} \rangle, \\ \langle \Delta n^2 \rangle &= \langle (\Delta n')^2 \rangle - \langle (\Delta n'_{\mathrm{N}})^2 \rangle. \end{aligned} \tag{8}$$

The value $\langle n \rangle$ may be equal to $(1/\hbar\omega) \cdot (\Delta \langle W' \rangle / \Delta Q')$ calculated by formula (3), yet in a general case $\langle n \rangle$ depends on $\Delta Q'$, but is absolutely independent of the number of resolution elements ΔQ of the entire optical system. Further, assuming the mean photon number $\langle n \rangle$ recorded at the optical system input and the variance $\langle (\Delta n)^2 \rangle$ to be prescribed, we seek their values at the output of the optical system. The variety of physical processes under consideration in this paper can be classified according to the value of the amplification coefficient K (see Table I).

3. CALCULATIONS OF $\langle n \rangle$ and $\langle (\Delta n)^2 \rangle$

To obtain analytical expression for the experimentally recorded quantities at $K \neq 1$ one needs to specify the type of brightness amplifier. However, in the limiting case of idealized amplifiers it is possible to obtain a fairly general expression for these quantities without specifying, for example, whether an amplifier active element has a one- or a two-quantum transition. The noise in such idealized amplifiers is produced only by zero-point and thermal fluctuations including both the vacuum electromagnetic field fluctuations and those of the dipole moment (for a laser amplifier), polarizability (for a Raman amplifier) or medium density (for a Brillouin amplifier). In the idealized amplifier case each transverse mode is started by zero-point fluctuations. The number of these modes having nearly equal gains in the amplifier cross-section area $\Delta S'$ will be characterized by

$$\Delta Q' = \frac{\Delta S'}{\lambda^2/\Delta\Omega}, \tag{9}$$

where $\Delta\Omega$ is the solid angle within which the angular spectrum of radiation passing through the amplifier is concentrated; $\lambda^2/\Delta\Omega$ is the transverse inhomogeneity scale of the field. In this case the photon number both at the amplifier input and output is expressed, according to (7), by the relation

$$n' = \frac{\lambda^2}{\Delta\Omega\hbar\omega} \int_{-\infty}^{+\infty} I' \mathrm{d}t, \tag{10}$$

or

$$n' = \Delta m'/\Delta Q', \tag{10'}$$

where

$$\Delta m' = (\Delta S'/\hbar\omega) \cdot \int_{-\infty}^{+\infty} I' dt$$

is the photon number on the area $\Delta S' = \Delta Q' (\lambda^2/\Delta\Omega)$.

The value of n' determined by formula (10a) describes the full photon number in the radiation passing through the amplifier cross-section, normalized to the full number $\Delta Q'$ of resolution elements in the cross-section, characterizing the transmission capacity of the optical system.

Thus introduced n' can be regarded also in a broader sense. Let us, for example, consider an optical system producing images of illuminated objects. In this case we can introduce a set of modes where each mode forms one resolution element in the image plane. When the amplifier is located near the diffraction-quality lens, and the object is rather far from the amplifier, these modes are, essentially, aperture-limited plane waves passing through the amplifier at different angles. The situation is different when the amplifier is placed near the image plane that coincides with the amplifier output end. Then, for a rather large aperture of the lens the corresponding modes are ray tubes diminishing along the amplifier length from the size of its diameter to the minimal size $(\lambda^2/\Delta\Omega)^{1/2}$ that characterizes a resolution element in the image plane. In both cases the maximum mode number is $\Delta Q'_{\max} = (\Delta S_{\mathrm{A}}/\lambda^2)\Delta\Omega$, where ΔS_{A} is the amplifier cross-section. Both sets of modes introduced in this case form an image of the object, and each mode changes its spatial structure by the diffraction laws. In the image plane these modes are focussed at the corresponding resolution elements, while in other planes they may overlap. Therefore, in the general case it is more precise to speak about modes with a transverse structure changing along the optical system axis, that form resolution elements in the image plane, rather than the resolution elements themselves. The notion of modes can be adopted not only for optical imaging systems, but others, too, such as holography, interferometry systems, etc.

Thus, the value of n' in formula (10a) can be regarded as the number of photons per mode. In this case formulae (5), (6) and (8) that relate the recorded values of the first and the second moments with the fields at the amplifier output can have a broader sense, that of relations between the photon numbers per mode at the optical system output (for example, in the image plane) and input (in the lens plane). It is clear that given this interpretation, the photon numbers at the projection optical system input coincide with the photon numbers $(\hbar\omega)^{-1} \cdot \Delta W/\Delta Q$ arriving from one resolution element (see (3)).

Direct calculations by formula (8) show that for an optical system involving an amplifier with the amplification coefficient K the mean photon numbers $\langle n(0) \rangle$ and $\langle n \rangle$ and their variance $\langle (\Delta n)^2 \rangle$ at the amplifier input and output are related for every mode by (the mode index is omitted for simplicity):

$$\langle n \rangle = K\eta \langle n(0) \rangle + (K-1)(\bar{N} + \bar{N}_{\mathrm{M}} + 1)\Delta f \cdot \tau, \tag{11}$$

$$\begin{aligned} \langle \Delta n^2 \rangle = {} & 2\eta \langle n(0) \rangle K \left[K\left(\bar{N} + \frac{1}{2}\right) + (K-1)\left(\bar{N}_{\mathrm{M}} + \frac{1}{2}\right) \right] \\ & + (K-1)(\bar{N} + \bar{N}_{\mathrm{M}} + 1) \\ & \times \left[(K+1)\left(\bar{N} + \frac{1}{2}\right) + (K-1)\left(\bar{N}_{\mathrm{M}} + \frac{1}{2}\right) \right] \Delta f\tau, \end{aligned} \tag{12}$$

where $\Delta f \cdot \tau$ is the normalized line width of the amplifier;

$$\bar{N}(T) = (\exp\frac{\hbar\omega}{k_B T} - 1)^{-1} \tag{13}$$

is the mean number of thermal photons in the ambient medium at temperature T;

$$\bar{N}_M(T_M) = (\exp\frac{\hbar\Omega}{k_B T_M} - 1)^{-1} \tag{14}$$

is the mean number of thermal optical or acoustic phonons with the frequency Ω in the medium of a Raman or Brillouin amplifier with a temperature T_M.

For a two-level (population inversion) laser amplifier $T_M \Rightarrow -T_M$ in formula (14), where $T_M = -\hbar\omega/k_B T \ln(N_2/N_1)$ is the negative temperature (for $N_2 > N_1$), N_1 and N_2 are the population concentrations of the lower and upper level, respectively.

The parameter η is the amplifier quantum efficiency characterizing the amplifier compatibility with the input signal. Its value is found by the formula

$$\eta = \frac{|\int \mathscr{E}_{opt}(t)\mathscr{E}^*(t)dt|^2}{\int|\mathscr{E}_{opt}|^2dt\cdot\int|\mathscr{E}|^2dt}, \tag{15}$$

where $\mathscr{E}_{opt}$ is the optimal structure of the input pulse field, providing maximum amplification of the pulse. The difference of the parameter η from one depends directly on the degree of mismatch between the input pulse frequency and length, and the amplifier line width Δf and switch-on time τ. This mismatch accounts for the fact that only a part of the input pulse energy excites the amplifier longitudinal modes corresponding to the fields with maximum amplification coefficients (their number is $\Delta f\cdot\tau$), while the rest of the energy goes to the modes that characterize the fields with low amplification coefficients. This degrades the quantum efficiency of the amplifier that is, essentially, a pulsed light beam receiver. The quantum efficiency can be expressed as $\eta = \hbar\omega/W_{min}$, where $W_{min} = W_{min}[\mathscr{E}(0)]$ is the input pulse energy per one transverse and one longitudinal mode of the amplifier; for this energy these modes are excited on the average by one photon of the input radiation. In other words, the parameter η describes the minimal photon number in the input pulse, required "to excite" a mode. For a complete match $W_{min} = \hbar\omega$ and $\eta = 1$. Without an amplifier ($K = 1$) η is also equal to 1.

In (12) the terms $\langle|\mathscr{E}^4|\rangle - \langle|\mathscr{E}^2|\rangle^2$ characterizing classical fluctuations of field $\mathscr{E}$ are omitted.

It follows from (11) and (12) that the mean photon numbers $\langle n\rangle$ and quantum variance $\langle(\Delta n)^2\rangle$ at the optical system output are sums of two components: one of them is connected with amplification of a coherent signal incident on the amplifier input, the other with the noise of spontaneous radiation or scattering.

4. EXAMPLES

Let us consider some specific cases.

A. *Amplifiers*

For $K \gg 1$ and $\bar{N}, \bar{N}_M \ll 1$ (the last condition is generally realized in a laser amplifier)

$$\langle n\rangle = K(\eta\langle n(0)\rangle + \Delta f\cdot\tau), \tag{16}$$

$$\langle(\Delta n)^2\rangle = 2K^2\left(\eta\langle n(0)\rangle + \frac{\Delta f\tau}{2}\right). \tag{17}$$

A relative variance is

$$\gamma = \frac{\langle(\Delta n)^2\rangle}{\langle n\rangle^2} = \frac{2[\eta\langle n(0)\rangle + (\Delta f\cdot\tau/2)]}{(\eta\langle n(0)\rangle + \Delta f\cdot\tau)^2}. \tag{18}$$

For $\eta\ \langle n(0)\rangle \ll \Delta f\cdot\tau$ γ tends to the classical limit $\gamma = 1/\Delta f\cdot\tau$. In the opposite limiting case the value $\gamma = 2/\eta\langle n(0)\rangle$ for $\eta = 1$ is twice as much as the value $\gamma = (1 + 2\bar{N})/\langle n(0)\rangle \approx 1/\langle n(0)\rangle$ describing the variance in the absence of amplification ($K = 1$).

The amplifier sensitivity (for $K \gg 1$) is determined by the relation

$$\langle n(0)\rangle > n_{min} = (1 + \bar{N} + \bar{N}_M)\frac{\Delta f\cdot\tau}{\eta}. \tag{19}$$

This formula does not depend on the type of amplifier and is valid both for one and for a succession of amplifiers, as well as amplifiers based on four-wave-mixing including those that provide phase conjugation of the amplified signal.

B. *Spontaneous radiation and scattering*

For $K - 1 \ll 1$, $\langle n(0)\rangle = 0$ the mean photon numbers are:

$$\langle n\rangle = \begin{cases} \sigma N_2 L\Delta f\cdot\tau & \text{—spontaneous radiation (laser amplifier)} \\ gIL\Delta f\cdot\tau & \text{—spontaneous scattering (Raman amplifier } k_B T_M/\hbar\Omega \ll 1), \\ gIL(k_B T_M/\hbar\Omega)\Delta f\cdot\tau & \text{—spontaneous scattering (Brillouin amplifier } k_B T_M/\hbar\Omega \gg 1). \end{cases} \tag{20}$$

Here σ is the amplifier cross-section, L the amplifier length, $K = \exp[\sigma(N_2 - N_1)L]$, g is the local gain of stimulated Raman or Brillouin scattering, I is the intensity of a pump wave in the amplifiers based on the stimulated scattering effects.

Consequently, the variance $\langle(\Delta n)^2\rangle$ is determined by the formula:

$$\langle(\Delta n)^2\rangle = \begin{cases} \sigma N_2 L\Delta f\cdot\tau = \langle n\rangle & \text{—spontaneous radiation (laser amplifier)} \\ gIL\Delta f\cdot\tau = \langle n\rangle & \text{—spontaneous scattering (Raman amplifier)} \\ gIL\dfrac{k_B T_M}{\hbar\Omega}\left(1 + gIL\dfrac{k_B T_M}{\hbar\Omega}\right)\Delta f\cdot\tau & \\ \quad = \langle n\rangle + \dfrac{\langle n\rangle^2}{\Delta f\cdot\tau} & \text{—spontaneous scattering (Brillouin amplifier)} \end{cases} \tag{21}$$

While for spontaneous radiation and spontaneous Raman scattering the statistics is purely quantum, it is classical for the Brillouin scattering at $gIL\, k_B T_M/\hbar\Omega \gg 1$, because if the latter condition is fulfilled, the number of scattered photons per one transverse and one longitudinal mode significantly exceeds unity.

C. *Absorbing media*

In this case $K \ll 1$. For thermodynamic equilibrium ($T = T_M$)

$$\frac{N_2}{N_1} = \exp(-\hbar\omega/k_B T),$$

$$\langle n \rangle = \langle (\Delta n)^2 \rangle = 0.$$

If this condition is absent, for example, the ambient temperature $T = 0$ and the absorbing medium temperature T_M is different from zero, formulae (11) and (12) yield the expressions for radiation of a black body:

$$\langle n \rangle = \frac{\Delta f\tau}{\exp(\hbar\omega/k_B T_M) - 1}, \tag{22}$$

$$\langle (\Delta n)^2 \rangle = \frac{\exp(\hbar\omega/k_B T_M)\Delta f\cdot\tau}{[\exp(\hbar\omega/k_B T_M) - 1]^2} = \langle n \rangle + \frac{\langle n \rangle^2}{\Delta f\cdot\tau}. \tag{23}$$

It is seen from (22) and (23) that for $k_B T_M \gg \hbar\omega$ the variance $\langle (\Delta n)^2 \rangle \approx \langle n \rangle^2/\Delta f\cdot\tau$ becomes classical, since the number of thermal photons per one transverse and one longitudinal mode is much larger than 1.

5. CONDITIONS FOR ACHIEVING THE QUANTUM SENSITIVITY LIMIT

Let us now consider the possibilities for reaching the quantum sensitivity limit n_{min} (see (19)) in a specific optical system that consists of laser amplifiers and a PC-mirror involving four-wave interaction of light with supersound.[3,4] A PC-mirror is a helpful tool when it is necessary not only to amplify radiation, but also to correct the aberrations induced by active elements. Besides, threshold-free four-wave PC mirrors generally have rather narrow spectral lines. In particular, a four-wave hypersonic phase conjugation mirror (FWHM) line is, as a rule, no more than 0.01 cm^{-1} for the switch-on time of 10^{-8}–10^{-7} s. The frequency band $\Delta f\cdot\tau$ of a FWHM is relatively narrow. Therefore, application of these PC mirrors significantly upgrades the sensitivity of optical systems. Thus, a signal wave energy in one spatial (transverse) mode for a FWHM must be larger than the value $W_{min} = \hbar\omega\, \bar{N}_M\, \Delta f\cdot\tau$ determined by the mean number of thermal phonons at a hypersonic frequency Ω and a dimensionless frequency band $\Delta f\cdot\tau$ of a PC-mirror (for $\eta = 1$). This formula follows from (19) for $N_M = k_B T_M/\hbar\Omega \gg 1$.

The limit set by the thermal noises can be overcome if a low-energy signal wave is pre-amplified so that the photon number in this wave at a PC-mirror input exceeds the total number of thermal phonons in the corresponding transverse mode. However, a quantum amplifier superluminescence noise is mixed in the signal during amplification; normalized to the input, its value is approximately equal to one photon per mode (see (19)) for $\bar{N}, \bar{N}_M \ll 1$). If $K > \bar{N}_M$, it is the superluminescence noise reflected by the PC mirror in the frequency band Δf that restricts the signal minimal energy at the amplifier input to the values $W_{min} = \hbar\omega\, \Delta f\cdot\tau$ (for $\eta = 1$).

To reach the quantum limit for the minimum energy of a signal subjected to PC let us consider whether it is possible to combine a four-wave hypersonic PC mirror and a double-pass quantum amplifier in one optical system.

For the arrangement when a quantum amplifier is placed before a PC-mirror we need to distinguish three additive components of noise radiation:

1. The PC-mirror intrinsic noise amplified in one pass of the radiation through the quantum amplifier. Its value depends on the type of the PC-mirror. Thus, for a FWHM under the optimal experimental conditions the source of noise is the backward scattering of a high-power pump pulse by thermal phonons near the exit end of the cell containing a nonlinear medium.

High values of the reflectivity R for this mirror are obtained for operation in the regime of absolute instability. Under these conditions conjugated wave power typically grows exponentially in time, and the number of longitudinal modes $\Delta f\cdot\tau$ in the noise radiation is consequently close to one. The PC-mirror noise energy per one transverse mode after the radiation passes through the quantum amplifier can be estimated in this regime from the formula

$$W_1 = \hbar\omega\cdot\bar{N}_M K R \Delta f\cdot\tau. \tag{24}$$

Under absolute instability the dimensionless band $\Delta f\tau$ is close to one, and the PC-mirror noise radiation, unlike the quantum amplifier superluminescence noise, is space-coherent, i.e., has a distinct speckle-inhomogeneous transverse field structure.

2. The quantum amplifier superluminescence noise initiated at the amplifier input, amplified in the frequency band Δf_A, reflected by the PC-mirror and then amplified again on its way back through the amplifier. This noise can be called a "double-pass" noise. Usually the amplifier frequency band Δf_A significantly exceeds the PC-mirror band Δf, and each component of the superluminescence noise, propagating within the PC-mirror angle of view, is reflected by this mirror with a narrower spectrum. If phase conjugation proceeds under absolute instability, the reflected superluminescence noise statistics changes due to the frequency band narrowing and shorter pulse length yielding a space-coherent noise radiation, and the dimensionless band $\Delta f\tau$ is close to 1. During the reverse pass through the amplifier this radiation has a speckle-inhomogeneous transverse field structure. The double-pass noise energy per one transverse mode (or resolution element) is roughly estimated in this case by the formula

$$W_2 = \hbar\omega\cdot K^2 R \Delta f\cdot\tau. \tag{25}$$

3. A broad-band "single-pass" noise of the amplifier superluminescence, initiated at the amplifier side facing the PC-mirror and increasing the direction of the conjugated wave propagation. The energy of this noise, calculated for one transverse mode, is

$$W_3 = \hbar\omega\cdot K\Delta f_A\cdot\tau_A, \tag{26}$$

where $\Delta f_A\cdot\tau_A$ is the number of longitudinal modes in the noise, τ_A the duration of a "single-pass" pulse of superluminescence.

Since noise is amplified in an ordinary and not a superregenerative quantum amplifier, a single-pass noise is non-

coherent by its statistics. A speckle-inhomogeneous transverse structure of such radiation changes over the characteristic time $1/\Delta f_A$. Therefore, the transverse distribution of the single-pass noise energy density becomes homogeneous over the recording time that largely exceeds $1/\Delta f_A$, without bright spots.

Let us estimate the minimal photon number n_{min} in a signal wave whose phase conjugation can be recorded in the scheme under consideration. Assuming the ratio of the output signal energy $W = K^2RW(0)$ to the total energy of all noise components to be equal to 1, we find the minimal number of all photons per one transverse mode:

$$n_{min} = \frac{W_1 + W_2 + W_3}{\hbar\omega \cdot K^2 R\eta} = \frac{R\bar{N}_M \Delta f \cdot \tau + RK\Delta f \cdot \tau + \Delta f_A \cdot \tau_A}{RK\eta}. \quad (27)$$

For $K \gg \bar{N}_M$ and $KR \gg \Delta f_A \tau_A$ the theoretical limit of the value $n_{min} = \Delta f\tau/\eta$, i.e., for a sufficiently large amplification coefficient one can reach the quantum sensitivity limit of an optical system, determined by formula (19). It is in this case that the formulae for an "idealized" amplifier considered above hold true.

6. FOUR-WAVE MIRRORS BASED ON HYPERSOUND TO PERFORM PHASE CONJUGATION OF LOW-ENERGY RADIATION

PC-mirrors used in projection optical systems for imaging of diffusely-scattering objects must meet the following requirements:

1. have a rather large number of resolution elements that coincides with the ratio of the PC-mirror angle of view θ to its angular resolution θ_g:

2. perform phase conjugation of low-energy radiation;

3. have a high reflectivity into a phase-conjugated wave.

These requirements are best met by PC-mirrors involving four-wave interaction of light and a hypersonic wave.[3,4] In this process two counterpropagating pump waves $\mathscr{E}_0^+$ and $\mathscr{E}_0^-$ (Fig. 2) with different intensities (for example, $|\mathscr{E}_0^-|^2 \gg |\mathscr{E}_0^+|^2$) and frequencies ω_0^+ and ω_0^- are transmitted through a stimulated-Brillouin-scattering-active medium. The frequency $\omega_1^+ = \omega_0^- - \Omega$ of the signal wave $\mathscr{E}_1^+$ undergoing PC is shifted relative to the frequency of the pump wave interfering with $\mathscr{E}_0^-$ by the value Ω which is equal to a Brillouin shift in the medium. Interference of waves $\mathscr{E}_0^-$ and $\mathscr{E}_1^+$ leads to a resonance excitation in the medium of a running hypersonic wave $Q \sim \mathscr{E}_0^- \mathscr{E}_1^{+*}$. The scattering of the second pump wave by this hypersonic wave produces a conjugate wave $\mathscr{E}_1^- \sim \mathscr{E}_0^+ Q \sim \mathscr{E}_0^+ \mathscr{E}_0^- \mathscr{E}_1^{+*}$ at the anti-Stokes (relative to wave $\mathscr{E}_0^+$) frequency $\omega_1^- = \omega_1^+ + \Omega$.

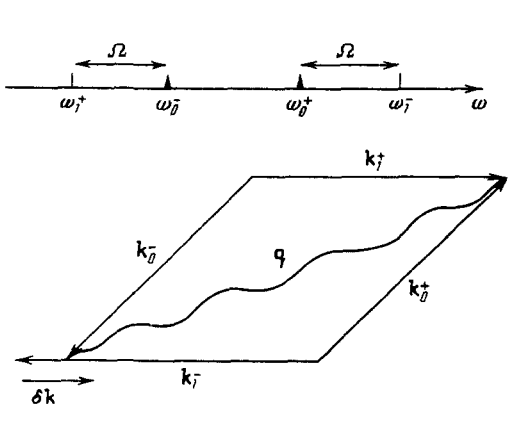

FIG. 2. Diagram of frequencies and wave vectors for four-wave mixing of light waves with a hypersonic wave: $\mathbf{k}_1^{\pm}$—are the wave vectors of the signal and the conjugate waves; $\mathbf{k}_0^{\pm}$—are the wave vectors of pump waves; $\mathbf{q}$—is the wave vector of the hypersonic wave; $\delta\mathbf{k}$—is the wave mismatch; $\omega_{0,1}^{\pm}$—are the frequencies of the interacting light waves; Ω—is the hypersonic wave frequency.

The opposite situation is also possible, when the anti-Stokes wave is actually the signal, and the Stokes wave is a conjugate wave. It is easily shown that in the absence of saturation effects the reflectivities into the PC-wave are equal in these situations

$$|\mathscr{E}_1^-(0)|^2/|\mathscr{E}_1^+(0)|^2 = |\mathscr{E}_1^+(L)|^2/|\mathscr{E}_1^-(L)|^2. \quad (28)$$

There are several reasons why it is possible to meet the above requirements using this interaction.

First, an important peculiarity of this process is that the waves interact effectively only when the signal wave frequency is shifted relative to the pump wave frequencies. This factor ensures high sensitivity of FWHM, since the spurious components of pump waves in this case (for example, related to their imperfect PC) do not form a background whose amplification could affect the signal and conjugated waves. Hence, the FWHM sensitivity is limited only by the level of spontaneous Brillouin scattering of pump waves in the medium.

Besides, if this interaction occurs under the conditions of absolute instability,[5,6,7] phase conjugation may proceed with a high ($R \sim 10^6$) reflectivity limited only by the pump waves saturation effects. In this case a PC-mirror is essentially a high-reflectivity nonlinear-optical amplifier.

Let us briefly discuss the conditions for reaching a FWHM limiting sensitivity.

It can be easily shown that for a FWHM this is possible only in a scheme with a Stokes signal wave $\mathscr{E}_1^+$. Indeed, stimulated scattering in the field of two counterpropagating light waves $\mathscr{E}_0^+$ and $\mathscr{E}_0^-$ with unequal intensities ($|\mathscr{E}_0^-|^2 > |\mathscr{E}_0^+|^2$) gives rise to the Stokes— (propagating towards wave $\mathscr{E}_0^-$) and anti-Stokes (towards wave $\mathscr{E}_0^+$) components. This simulated scattering is induced by spontaneous scattering of wave $\mathscr{E}_0^-$ near the nonlinear medium boundary $z = 0$ into the Stokes component $e_s(0)$ of frequency $\omega_1^- - \Omega$, and by the scattering of wave $\mathscr{E}_0^+$ at the boundary $z = L$ into the anti-Stokes component $e_a(L)$ of frequency $\omega_0^+ + \Omega$. The scattered waves amplitudes at the output boundaries of the medium $e_s(L)$ and $e_a(0)$ are related in the absence of saturation effects to their amplitudes at the input boundaries as

$$e_s(L) = K_s^A e_s(0) + R_s^A e_a(L), \quad (29)$$

$$e_a(0) = K_a^A e_a(L) + R_a^A e_s(0),$$

where the coefficients K_s^A and K_a^A can be treated as amplification coefficients of the corresponding waves (with regard to the amplitude), and $R_s^A = R_a^A = R^A$ as the coefficient of mutual rescattering of the Stokes wave into the anti-Stokes wave and back (amplitude reflectivities into the conjugated wave). In our situation $|K_s^A|^2 > |R^A|^2 > |K_a^A|^2$.

We now assume that besides a seed wave at the boundary $z = 0$ there is also a Stokes signal wave $\mathscr{E}_1^+(0)$. Then,

the PC-mirror-reflected wave amplitude is

$$K_a^A e_a(L) + R^A(e_s(0) + \mathscr{E}_1^+(0)). \quad (30)$$

Since $|R^A|^2 > |K_a^A|^2$, the minimal intensity of the signal wave is limited by the value $|e_s(0)|^2$, i.e., it is determined by the level of spontaneous scattering of the pump wave $\mathscr{E}_0^-$.

For the anti-Stokes signal wave $\mathscr{E}_1^-(L)$ the phase-conjugated wave amplitude is

$$K_s^A e_s(0) + R^A(e_a(L) + \mathscr{E}_1^-(L)). \quad (31)$$

Since $|K_s^A|^2 > |R^A|^2$, the signal wave intensity is found from the condition

$$|\mathscr{E}_1^-(L)|^2 > (|K_s^A|^2/|R^A|^2)|e_s(0)|^2 > |e_s(0)|^2. \quad (32)$$

Thus, in a scheme with a Stokes signal wave the PC-mirror sensitivity is determined by the energy of the Stokes-frequency noise due to spontaneous scattering of a pump wave. Normalized to one transverse mode (which for a projection optical system corresponds to one resolution element) and calculated for the medium input (see (11) for $\langle n(0)\rangle = 0$, $\bar{N}_M \gg 1$), this energy is equal to

$$W_M = \hbar\omega \cdot \bar{N}_M \Delta f \cdot \tau. \quad (33)$$

Hence, the minimal energy of the signal wave per one transverse mode (resolution element) is

$$W_{min} = W_N/\eta = \hbar\omega \cdot \bar{N}_M \Delta f \cdot \tau (1/\eta), \quad (34)$$

where the parameter η is similar to quantum efficiency and is determined by formula (16). The dimensionless frequency band $\Delta f \cdot \tau$ of FWHM amplification can be close to one. In this case a four-wave mirror is, actually, a narrow-band pulsed amplifier, and the parameter η depends on how well the signal pulse arrival time and the pulse frequency spectrum correspond to the frequency band Δf and the PC-mirror amplification time τ.

Now we shall briefly discuss the problem of the parameter $\Delta f \cdot \tau/\eta$ minimization, because only in this case it is possible to achieve limiting sensitivity of FWHM and, consequently, the limiting sensitivity of the FWHM—quantum optical amplifier scheme considered in Section 5.

The value of $\Delta f\tau$ depends on the character of the interaction of the waves in a FWHM. In the convective instability region (below the absolute instability threshold) η may be close to 1, and the dimensionless band $\Delta f \cdot \tau$ is determined by the length of the pump wave pulses and the stimulated scattering frequency band. In the absolute instability region due to the time-exponential growth of both the amplified signal and the conjugated wave amplitudes, only a part of the initial radiation noise is amplified, the one with the length τ_0 of the order of the characteristic time of the scattered waves growth. The PC-mirror frequency band is determined by the same parameter $\Delta f \sim 1/\tau_0$. Hence, the dimensionless band $\Delta f \cdot \tau$ in the absolute instability region can be close to 1 (at least, for a slight excess of the pump wave power over the threshold).

The value of $\Delta f \cdot \tau$ typical for a FWHM can be estimated from measurements of the relative variance $\gamma = \langle \Delta w^2 \rangle / \langle w \rangle^2$ of the energy density fluctuations in the noise radiation excited by stimulated scattering of the counterpropagating light waves by the hypersonic wave (angular brackets here mean averaging over a beam cross-section). To this end it is necessary to express γ in terms of the dimensionless band $\Delta f \cdot \tau$, i.e., in terms of the characteristic number of the orthogonal-in-time coherent modes forming the FWHM noise.

For this we expand the complex amplitude of noise radiation at the FWHM output in the Karunen–Loev series (with the minimal remainder term in the case of a finite number of the expansion terms):[2]

$$E = \sum_{n=1}^{\infty} e_n(r_\perp)\varphi_n(t). \quad (35)$$

Each term in this series is orthogonal not only in time ($\int_{-\infty}^{+\infty} \varphi_n(t)\varphi_m^*(t)dt = \delta_{nm}$), but also with respect to the transverse coordinates ($\int_{-\infty}^{+\infty} e_n(\mathbf{r}_\perp) \times e_m^*(\mathbf{r}_\perp) d^2 r_\perp = \lambda_m \delta_{mn}$). The number of the expansion terms that are major energy contributors is bounded from above by the minimum of the characteristic number of longitudinal $\Delta f \cdot \tau$ and transverse (θ^2/θ_g^2) modes.

Under the experimental conditions $\Delta f \cdot \tau \ll \theta^2/\theta_g^2$, therefore, the characteristic number of terms in expansion (35) is determined by the value of $\Delta f \cdot \tau$. Taking into account the energy density

$$w = \text{Const.} \int_{-\infty}^{+\infty} |\mathscr{E}|^2 dt$$

we find:[2]

$$\gamma = 1/N_{eff}, \quad (36)$$

where

$$N_{eff} = \left(\sum_{n=0}^{\infty} \lambda_n\right)^2 \left(\sum_{n=0}^{\infty} \lambda_n^2\right)^{-1}$$

is the effective number of terms in the expansion (35), nearly equal to $\Delta f\tau$. (We here skip more detailed calculations that directly relate the minimal signal energy W_{min} in (19) to N_{eff}. In its turn N_{eff} depends on the FWHM operation and is roughly determined by the product of the FWHM frequency band Δf by the characteristic length of the reflected pulse τ). In this way measurements of γ allow one to estimate $\Delta f \cdot \tau$ by the formula $\Delta f \cdot \tau = 1/\gamma$.

The experimental value of $\Delta f \cdot \tau$ was obtained for FWHM under absolute instability for a relatively large number of the transverse modes ($\theta/\theta_g \approx 600$), using measurements of relative fluctuations of the energy density in the speckle-inhomogeneous noise radiation of a PC-mirror in the absence of a signal wave.[8] We measured the ratio of the energy density in an arbitrary area of a much smaller size than the characteristic size of speckle-inhomogeneity of the noise radiation transverse structure, to the cross-section-averaged energy density. The measured ratio was averaged over the results of several experiments for the same energy of the pump waves. It turned out (see Ref. 8) that $\gamma \approx 0.5$, and so $N_{eff} = \Delta f \cdot \tau \approx 2$.

However, reaching the quantum efficiency $\eta \simeq 1$ in the absolute instability conditions is a rather complicated problem. This regime sets in due to a π-shift of the reflected (anti-Stokes) wave phase with respect to the hypersonic wave phase over the length of the nonlinear medium, and this results in positive feedback. This phase shift occurs due to a wave mismatch $\delta k \cdot L$ or detuning of the signal wave frequency ω_1^+ from perfect resonance by some value

$\Delta\Omega = \Omega - (\omega_0^- - \omega_1^+)$. In this case each value of the wave mismatch over the nonlinear medium length $\delta k \cdot L$ has a corresponding value of the signal wave detuning $\Delta\Omega$; the absolute instability threshold is minimal and, hence, the scattered waves increment is maximal for this detuning.[9] Since the noise radiation associated with spontaneous scattering that is mixed with the signal wave has quite a broad frequency band, the sensitivity limit and the value $\eta \approx 1$ can be obtained only on condition of a complete match between the light wave frequency ω_1^+ and the parameter $\delta k \cdot L$. In particular, if the conditions of a perfect Brillouin resonance are realized in an experiment (in this case the frequency of the signal wave produced, for example, by scattering in the same medium that is used for a FWHM, is Brillouin-shifted by Ω), the value $\Delta\Omega = 0$ will correspond to $\delta k \cdot L \approx 5 - 6$ (Ref. 9).

Another important condition for achieving high quantum efficiency values ($\eta \approx 1$) is the necessity for agreement between the time of the signal wave arrival in FWHM with the FWHM switch-on time, i.e., when the pump waves enter the nonlinear medium. For operation under absolute instability, due to growth of the scattered waves amplitudes in time, the highest amplification is achieved only by that part of the input pulse that enters the nonlinear medium right after the pump waves pass over the instability threshold. The amplification time for the following part of the signal pulse is shorter and so is the degree of amplification here, hence the energy of this part has a weak influence on the energy of the FWHM-reflected radiation.

The numerical calculations performed for the Gaussian (in time) pulses of a signal wave and pump waves show that the quantum efficiency value will reach its peak when the signal wave pulse maximum coincides with the moment the pump waves reach the absolute instability threshold, and the signal pulse duration is 2–4 times longer than the attenuation time of a hypersonic wave.

The above requirements having been met, we managed to obtain in Ref. 10 the sensitivity of a FWHM–based projection optical scheme close to the theoretical limit (33) for the brightness amplification coefficient $R \approx 10^6$ and the linear number of resolution elements in the field of view $\theta/\theta_g \approx 600$.

7. PROJECTION OPTICAL SYSTEM FOR AMPLIFICATION AND RECORDING OF WEAK OPTICAL RADIATION

The possibility of reaching the quantum sensitivity limit in amplification of optical radiation that transfers object images with a large number of resolution elements was studied experimentally for a projection optical system involving Nd-glass laser amplifiers in combination with FWHM. Application of quantum amplifiers in such systems sets certain requirements on the amplifiers themselves and on the entire system. Along with a high amplification coefficient, these quantum amplifiers must be capable of transmitting a large number of transverse modes and providing a uniform gain within the field of view. These requirements are contradictory, since a wide angle of view for a laser amplifier degrades the latter's efficiency due to amplification of spontaneous radiation, spurious generation induced by the reflection of radiation at different optical elements that form images, and some other factors.[16,17]

As shown in Section 5, the amplification coefficient value K in the considered optical scheme must significantly exceed the mean number of thermal phonons $\bar{N}_M$ in a phase-conjugation mirror medium. For the experimental conditions of Refs. 10–12 and the ambient temperature we have $\bar{N}_M = 2.5 \cdot 10^3$ (a $TiCl_4$ PC-mirror, $\Omega = 2 \cdot 10^{10}$ rad/s).

Besides, the Fresnel number of a laser amplifier $d^2 n/\lambda L$ (here d is the amplification medium transverse size, L is its length, n the refractive index) that defines the number of transverse modes transmitted through the amplifier and coincides with the ratio of the amplifier angle of view θ to the diffraction resolution θ_a, must be large enough—generally, $d^2 n/\lambda L = \theta/\theta_g > 10^2$.

The required conditions are most easily realized in multi-cascade amplifiers providing successive transfer of image from one active element to another.[16,17] An example of such a scheme used in Refs. 11, 12 is given in Fig. 3. The object plane A illuminated by a laser pulse ($\lambda = 1.054$ mcm, pulse length $5 \cdot 10^{-8}$ s) is projected by lens *1* onto the output boundary of a two-cascade laser amplifier consisting of two identical active elements ($d = 10$ mm, $L = 300$ mm) with a retransmitter (lenses *3,4*) between them. It follows from Ref. 1 that such an optical scheme (lens positioned at the input end of the active element and projecting the object plane onto the image plane at the end of the output active element) optimizes the energy coefficient of field transfer from one limited aperture to another.

The value of the unsaturated amplification coefficient $K_0 = (1.8–2) \cdot 10^2$ was uniform over the cross-section in each cascade. This provided the required value of $K = K_0^2$ for the same number of resolution elements (θ/θ_g) ≈ 350 determined by the geometrical dimensions of one amplifier.

After the quantum amplifiers the radiation was incident

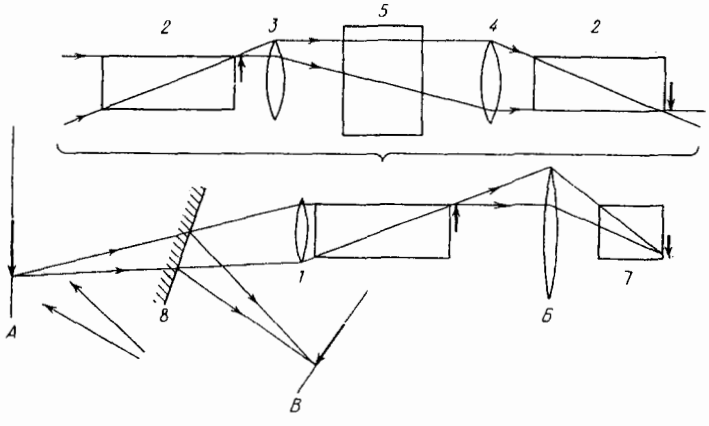

FIG. 3. Experimental setup: *1*—lens; *2*—Nd-glass quantum amplifier; *3,4*—optical transducer lenses; *5*—Faraday isolator; *7*—PC-mirror; *8*—semi-transparent mirror; *A*—object plane illuminated by laser beam; *B*—image plane.

on the PC-mirror 7. An optimal combination of amplifiers and a phase-conjugation mirror can be achieved by placing one more optical retransmitter between them to transfer a suitably scaled image of the amplifier to the FWHM. But, since the number of resolution elements of PC-mirror $(\theta/\theta_g)_M = 600$ exceeded the corresponding amplifier parameter $(\theta/\theta_g)_A$, only one lens 6 was used in the experiment, which projected the laser amplifier boundary image on the PC-mirror boundary.

The PC-reflected radiation once again passed through the quantum amplifiers, split into two branches by the semitransparent mirror 8 and then recorded in the image plane B that is optically conjugate the plane A.

In calculations of such schemes with a high amplification coefficient for the input signal one should take into account the fact that the value of the amplified quantum noise becomes quite large even in the absence of a signal wave and can facilitate saturation of laser amplifiers and even their optical breakdown. Indeed, the energy of the amplifier superluminescence noise starting at the amplifier input, reflected by the PC-mirror and amplified again during a reverse pass through the amplifier, according to (25), is $\hbar\omega K^2 R\Delta f\cdot\tau$. To achieve quantum sensitivity, the value of K must satisfy the condition $K > 10^4$ (see above).

Another condition for achieving the limiting sensitivity in this scheme (see Section 5) is $KR \gg \Delta f_A \tau_A$. For a neodimium amplifier the value of the dimensionless band $\Delta f_A \tau_A$ determined by the line width of amplification and the lifetime of the upper operating level is $\Delta f_A \cdot \tau_A \approx 10^{10}$. For $K \approx 10^4$ this sets the requirement $R \approx 10^6$. Hence, the value of the superluminescence amplified noise energy for $\lambda = 1$ and $K \sim 10^4$, $R \approx 10^6$ is of the order of $2\cdot 10^{-5}\ \Delta f\cdot\tau$ [J] per each transverse mode. The noise total energy proportional to the number of transverse modes $(\theta/\theta_g)^2$ for $\theta/\theta_g \sim 10^2$–$10^3$ proves to be equal to units or tens of joules even if each transverse mode is excited by one photon ($\Delta f\cdot\tau = 1$). To prevent saturation of a quantum amplifier one has to reduce the amplification coefficient over a second pass through the amplifier. To this end we used Faraday isolator 5 (see Fig. 3) that attenuated the radiation by a factor of $2\cdot 10^2$ in the second pass through the quantum amplifiers. Under these conditions the total gain for a double-pass projection system reached 10^{11}–10^{12}.

8. ANGULAR RESOLUTION, ANGLE OF VIEW AND SENSITIVITY OF A PROJECTION SYSTEM

An experimental study of the angular resolution and reflectivity of a projection system, depending on the angular position of the source in plane A relative to the optical axis was carried out by photographing the source image in PC rays through an autocalibration mirror wedge, which was followed by photometering, and also by measuring the conjugated radiation energy. A "point" source of radiation was initiated in plane A in this case by focusing the illumination radiation into a spot of a much smaller size than a resolution element.

Figure 4 gives the dependence of the angular resolution θ_g normalized to the angular resolution $\theta_g(0)$ in the center of the field of view on the angle φ that coincides with the angular shift of the "point" source and is normalized to the value $1.22\,\lambda/d$. The obtained value of θ_g coincides within experimental accuracy with the value determined by the diffraction limit for a circular diaphragm of diameter $d = 9.5$ mm (the light diameter of the quantum amplifier active element).

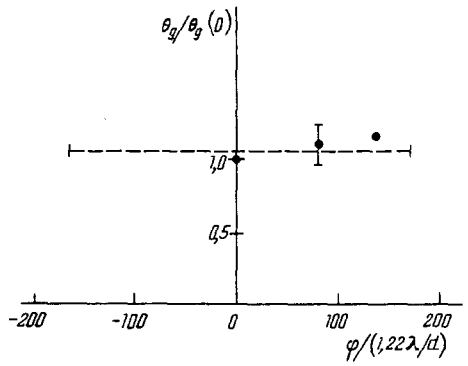

FIG. 4. Dependence of the angular resolution θ_g, normalized to $\theta_g(0)$, on the angular position of the source φ normalized to the value $1.22\,\lambda/d$. Dashed line indicates the calculated dependence for the experimental geometry being used.

The full size of the field of view in plane A corresponds naturally to the size of the image of the amplifier end formed by lens 1 in plane A. Here the total amplification of the projection system, measured by the relative energy density of the amplified and PC-mirror-reflected noise radiation at different angles, turned out to be practically independent of φ within the entire field of view.

The considered scheme of image amplification was studied for limiting possibilities by measuring its sensitivity at the lowest possible levels of the energy density of the illumination radiation. The "object" to be recorded here was a laser beam (6 mm diameter) with a uniformly distributed intensity, aimed at a diffuse-scattering surface (milk glass) located in plane A.

The size of the recorded "spot" in the center of the field of view was much smaller than the full size of the field of view in plane A ($\sim$8.5 cm), but significantly exceeding the size of the resolution element ($\sim$240 μm) related to the limiting angular resolution of the optical scheme. The latter circumstance allowed for averaging of the energy density of both the noise radiation and the images recorded in plane B over their transverse speckle-inhomogeneous structure typical for coherent-light imaging schemes.

Images were recorded in plane B for different levels of the illumination radiation energy, maximum pumping of laser amplifiers and the FWHM pump wave energies corresponding to values nearly 1.5–2 times the absolute instability threshold.

To get the quantum efficiency η to be close to one and, hence, reach the limiting sensitivity of a projection system the FWHM pump wave pulses ($\tau_p = 50$ ns) and signal wave pulses ($\tau_s = 12$–15 ns) of different length were used in these experiments along with optimization of the signal wave arrival in FWHM.

Quantitatively the limiting sensitivity was estimated by measuring the value of the signal-to-noise ratio $\mathrm{SNR} = \Delta w_i(w)/\Delta w_N$, which in this case was equal to the ratio of the energy density Δw_i falling onto the image area to the energy density of eigen noise w_N (measured in the area adjacent to the image) for various values of the illumination energy density w.

Figure 5a gives the dependence of SNR on the signal

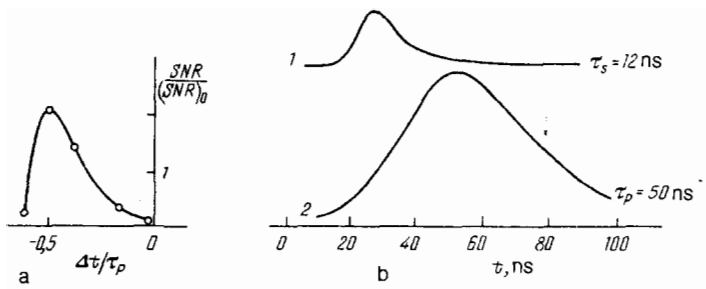

FIG. 5. a—dependence of the signal-to-noise ratio SNR on the signal wave time delay Δt; b—oscillograms of the signal wave (*1*) and pump waves (*2*) pulses for their optimal mutual position.

wave time delay Δt normalized to τ_p. In Fig. 5a the SNR value is normalized to the value $(SNR)_0$ corresponding to the case of a signal wave pulse with $\tau_s = \tau_p = 50$ ns and time delay $\Delta t = 0$.

In Fig. 5b there are oscillograms of the signal wave and pump wave pulses corresponding to their optimal relative position. Here we measured SNR for different densities of the illumination energy w in plane A. The corresponding dependence is given in Fig. 6. For comparison there is a similar dependence in the same figure, obtained under the same conditions except that the signal and the pump wave pulses were equal in length and coincided in time.

It follows from Fig. 6 that the projection system natural noises limit its sensitivity at $w_{min} = 1.4 \cdot 10^{-9}$ J/cm^2 (in the case of illumination of a diffusely scattering object).

Using the obtained w_{min} one can easily find the minimal energy arriving in the projection system from one resolution element. As shown above (see (3)), w and W_{el} are related (for scattering into the solid angle 2π) by $W_{el} = \lambda^2 w/8\pi$; this relation does not depend on the experimental scheme. Taking into account real characteristics of the scatterer being used (depolarization and a slightly nonuniform scattering diagram), we replace the coefficient $1/8\pi$ by $3 \cdot 10^{-2}$ (more details in Refs. 10, 11). Hence, we have

$$W_{el,min} = 4{,}8 \cdot 10^{-19} \text{ J} = 2{,}4\hbar\omega . \qquad (37)$$

Thus a near-theoretical limiting value of the sensitivity W_{el} was obtained in the experiment, since the value of the dimensionless band of amplification for FWHM (see above) is $\Delta f \cdot \tau \approx 2$.

9. THE EFFECT OF QUANTUM FLUCTUATIONS ON IMAGING

To study the fluctuations in the number of photons over the cross-section, a slot with a transverse size of 2–3 resolution elements was inserted in plane A of the projection optical system (see Fig. 3) and irradiated (in the direction of the receiving system) by a laser beam.[8] The slot image formed by the projection optical system was recorded by a calibrated matrix photodetector and computer-processed. Measurements of the relative variance of the energy density fluctuations along the slot were found to coincide with the relation $\gamma = \langle(\Delta n)^2\rangle/\langle n\rangle^2$, depending on the mean photon number per one transverse mode at the amplifier input $\langle n(0)\rangle$. For $\langle n(0)\rangle \to \infty$ (classical limit) the variance is related to speckle-inhomogeneous noises arising due to imperfect PC and is $\gamma_{cl} = 7 \cdot 10^{-3}$. This is a minimal value. When $\langle n(0)\rangle$ decreases, the value γ is supposed to be increasing and reach $\gamma = 1/\Delta f \cdot \tau$ in the absence of a signal (see (18)).

Processing of the energy density distributions in the slot image plane allowed us to determine the parameter γ as a function of $\eta\langle n(0)\rangle$ for a wide range of the argument variations up to values corresponding to the classical limit. Averaging was performed along the slot. The obtained results are given in Fig. 7. Here experimental values are marked by dots. They are compared with the solid curve theoretically constructed using formula (18) generalized for the case that takes into account also "classical" speckle-inhomogeneous noises caused by imperfect PC:

$$\gamma = \gamma_{cl} + \frac{2[\eta\langle n(0)\rangle + (\Delta f \cdot \tau/2)]}{(\eta\langle n(0)\rangle + \Delta f \cdot \tau)^2}. \qquad (38)$$

If we substitute the experimental values of the parameters

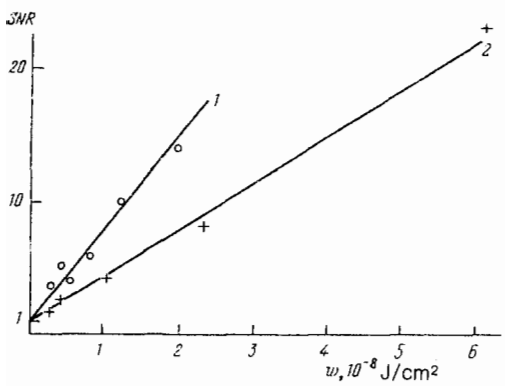

FIG. 6. Dependence of SNR on the illumination energy density w for different lengths of the signal- and pump waves pulses and their optimal mutual position (*1*), and for the case when these pulses coincide in time ($\tau_s = \tau_p$, $\Delta t = 0$) (*2*).

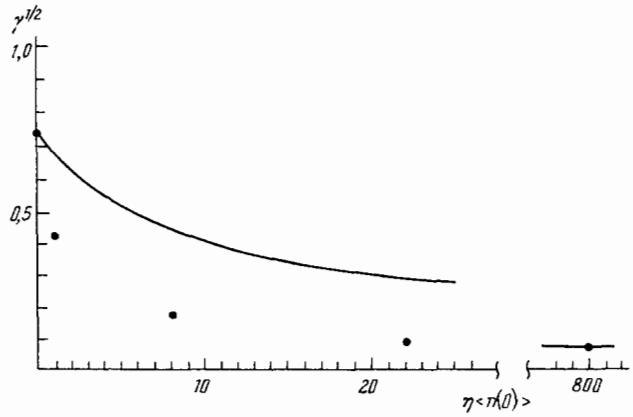

FIG. 7. Dependence of the relative variance $\gamma^{1/2}$ on the mean photon number per resolution element $\eta\langle n(0)\rangle$.

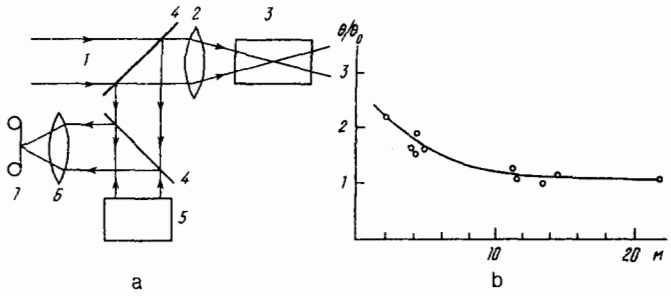

FIG. 8. a) Experimental scheme: *1*—single-mode laser beam; *2*—lens $F = 30$ cm; *3*—$TiCl_4$ cell; *4*—beamsplitting plates; *5*—projection optical system; *6*—lens; *7*—photodetector. b) Dependence of the Stokes wave divergence θ normalized to the divergence of a single-mode laser beam θ_0 on the Brillouin scattering increment M.

$\gamma = 7 \cdot 10^{-3}$ and $\Delta f \cdot \tau = 2$ entering this formula (see above), we will see that the tendency for γ variation with increasing $\langle n(0) \rangle$ is in qualitative agreement with the theoretical predictions (see the solid curve in Fig. 7).

10. APPLICATIONS

The above-described projection system can be used to record the spatial structure of a weak coherent radiation scattered in different media, including cases of coherent radiation against a higher-power noncoherent background. The experimental results obtained in the study of these possibilities[13] are given below.

We measured angular divergence of the Stokes radiation for Brillouin scattering of a single-mode transverse structure laser beam (pulse duration $\tau_p = 50$ ns, beam diameter $d = 10$ mm) focused into a scattering medium ($TiCl_4$) (Fig. 8). A four-wave PC-mirror of a projection laser system uses pump beam interaction with a signal wave undergoing PC, whose frequency is Stokes-shifted with respect to the frequency of the pump wave interfering with the signal; this shift is equal to the Brillouin shift in a FWHM medium. By using the same medium for both the four-wave PC-mirror and cell *3* in this case (Fig. 8a) we ensured an automatic "tuning" of the laser system frequency band to the Brillouin scattering frequency in cell *3*.

The experimental scheme is given in Fig. 8a. The radiation scattered in cell *3* was split by plate *4* and after amplification and PC in the laser projection system its angular structure was photographed in the lens focal plane. The Brillouin scattering increment in this case $M = kgP$ ($k = 2\pi/\lambda$; $g = 2 \cdot 10^{-2}$ cm/MW is the local increment; P is the initial beam power incident on cell *3*) varied from values corresponding to an active stimulated scattering regime to the values close to one, which is typical for a transition to spontaneous scattering operation. The dependence of the Stokes wave divergence θ normalized to the diffraction-limited divergence of initial radiation θ_0 on the increment M is given in Fig. 8b. Higher divergence of the scattered radiation with a decreasing M is accounted for by less discrimination of the Stokes waves with different transverse structure, which leads to violation of the PC conditions in transition to spontaneous radiation.

We have also recorded the spatial structure of scattered light in laboratory air. The frequency of the signal (probe) wave in this case shifted so that the scattered radiation was recorded at the nonshifted (relative to the probe radiation) frequency. The experimental scheme is given in Fig. 9 and Fig. 10 presents images of the transverse structure of the scattered radiation for the probe beam energy of $W_p \sim 2 \cdot 10^{-2}$ J, pulse length $\tau_p = 5 \cdot 10^{-8}$ s and for different angles between the probe beam direction and the optical axis of the system.

The experiments showed that the scattered radiation has the same polarization as the probe beam. This fact along with the scattering intensity estimate (see below) lead us to conclude that in this case we observe molecular scattering by thermal fluctuations of the medium density at a nonshifted frequency. It is known that according to the Landau–Placzek formula[14] the molecular scattering intensity at the nonshifted frequency is roughly equal to the intensity of the Brillouin component. Therefore, to estimate the intensity of this scattering we have used the data for the Brillouin scattering cross-section in nitrogen at $p = 1$ atm.

For molecular Brillouin scattering in this case the mean photon number in the scattered radiation per one transverse and one longitudinal mode is (see (20))

$$\langle n \rangle = M \bar{N}_M, \tag{39}$$

where $\bar{N}_M = k_B T_M / \hbar\Omega$ is the number introduced above of thermal phonons at the hypersonic wave frequency Ω equal to the Brillouin shift in air; T_M is the temperature; $M < 1$ is the Brillouin scattering increment. In this experimental geometry

$$M = g \int I(z, r_\perp) dl, \tag{40}$$

where $I(z, r_\perp)$ is the intensity distribution of the probe light beam focused in air, the integral being taken along the direction of observation. It is easily shown that for φ larger than the angle between the converging rays in the probe beam, for the focal waist area

$$M = kgP\varphi_0/\varphi, \tag{41}$$

with an accuracy up to a coefficient of the order of unity, where P and $\varphi_0 = d/F$ are the power and angle of convergence of the probe beam; d the diameter of this beam on the

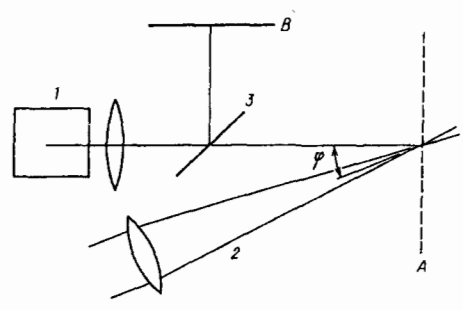

FIG. 9. Experimental scheme: *1*—projection optical system; *2*—probe laser beam; *3*—beamsplitting plate; *A*—object plane, *B*—image plane.

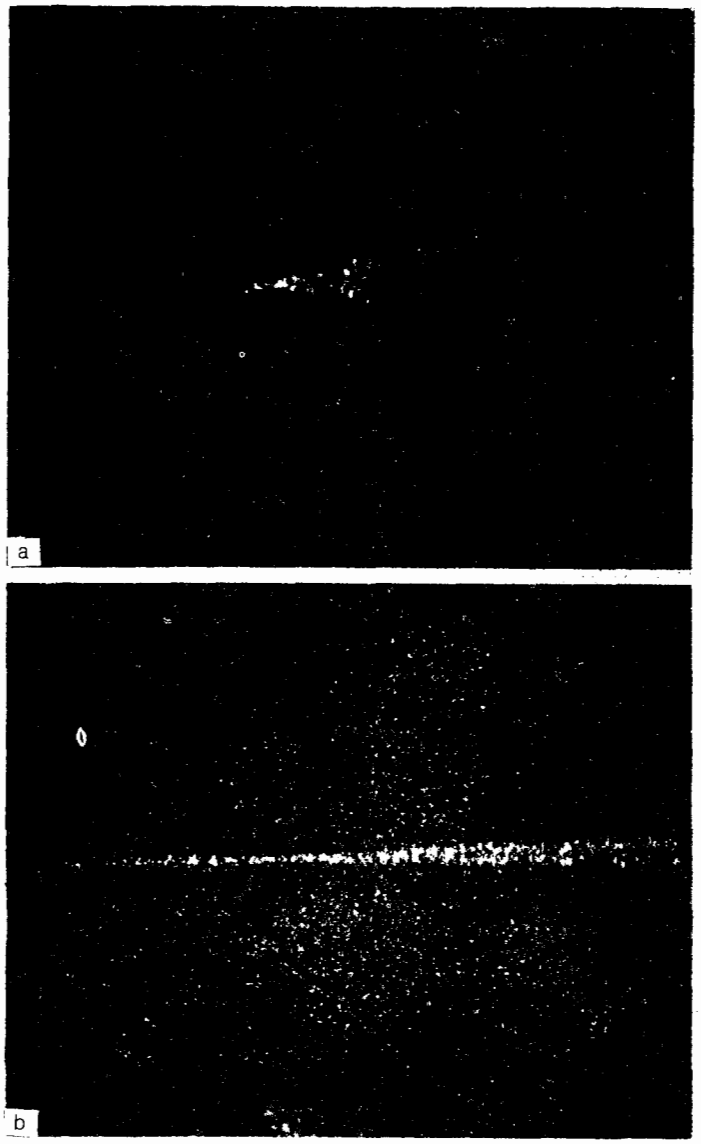

FIG. 10. Image of the transverse structure of scattered radiation for $\varphi = 5°$ (a) and $\varphi = 30°$ (b).

focusing lens with the focal length F. Thus, for the near-focal waist area we have

$$\langle n(0)\rangle = kgP(k_B T_M/\hbar\Omega)\varphi_0/\varphi. \quad (42)$$

By substitution of $k_B T_M/\hbar\Omega = 10^4, kgP = 25P/P_{th}$, where $P = W_p/\tau_p = 0.4$ MW; $P_{th} = 130$ MW [15] is the SBS threshold power in nitrogen at $p = 1$ atm, for $\varphi_0 = d/F = 1/300$ we find $\bar{n} = 2{,}6/\varphi$. The scattering process could be observed experimentally in the angle range from the minimal values ($\varphi = 7\cdot 10^{-3}$) up to $\varphi \approx 0.25$. For larger φ the scattering signal failed to stand out against the amplified quantum noises. Since the signal wave and pump wave pulses used in this experiment coincided in time, the minimum input signal per resolution element in the reception band $n_{min} \approx 5$ (Refs. 11,12). For the angle $\varphi = 0.25$ corresponding to a negligible excess of the scattered signal intensity over noise we have $\langle n(0)\rangle \approx 10$, which is close to n_{min}. Thus, the experimentally obtained energy is close to the theoretically predicted value.

Apart from a uniform (on the average) scattering some photographs revealed bright points corresponding to scattering by particles (dust, aerosol, etc). The total energy of this scattering can be comparable with or even higher than the energy of scattering by density fluctuations. In this case a projection optical system allows for separate observation with spatial resolution of scattering by particles and by density fluctuations.

The possibility of amplification and recording of molecular scattering an scattering by microparticles in air at such low energies of the probe radiation can be used for development of a coherent lidar to measure, for example, spatial distribution of wind velocity.

However, we studied another, relatively simple way of measuring the scattering medium velocity, which can be used when the velocity is relatively high.[13] This technique is based on measurements of the dependence of the magnitude of the scattered signal on the angle between the velocity vector of the scattering medium and the observation direction. Here the Doppler shift of the scattered radiation frequency, depending on the medium velocity and the indicated angle, makes is possible to determine the velocity within the accuracy of the reception system line width. In our case this is about 10^4 cm/s.

This technique was realized experimentally in measure-

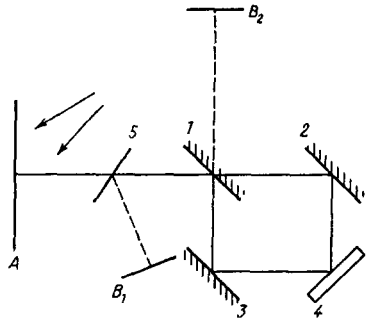

FIG. 11. Experimental scheme: *1*—semi-transparent mirror; *2,3*—mirrors; *4*—projection optical system; *5*—beamsplitting plate; *A*—object plane (diffuse-scattering surface) illuminated by laser radiation; B_1, B_2—image planes optically conjugate to plane *A*.

ments of a plasma jet velocity.[13] It is of essential importance that the plasma natural noncoherent glow is not recorded in this case due to the narrow band of the reception system.

This high-sensitivity projection system allowed us also to observe interest of extremely weak waves with a complicated spatial structure. The experimental scheme is given in Fig. 11. A laser pulse with a uniform intensity distribution was directed at a diffuse-scattering surface (milk glass) placed in the object plane *A*. Next, a signal wave (radiation scattered by the diffuse surface) was split by a semi-transparent mirror 1 into two beams which were then recombined and reflected with a simultaneous PC from a projection optical system. After the reflected beams of fairly high energies were combined at mirror 1 producing an image in planes *B* 1 and *B* 2 conjugate to the object plane *A*. The signal-to-noise ratio $\mathrm{SNR} = \Delta w_i(w)/\Delta w_N$ was measured in these planes as a function of the illumination energy density w in the scattering plane, using the technique described in Sect. 8. As stated above, the value of w fully determines (for recorded images with diffraction resolution) the mean energy (photon number) $\langle n(0)\rangle$ arriving in the recording system from one resolution element.

Figure 12 gives the dependences of the SNR values in plane *B* 1—$(\mathrm{SNR})_1$ and *B* 2—$(\mathrm{SNR})_2$.

In Fig. 12 line *1* is the behavior of $(\mathrm{SNR})_1$ in channel 1

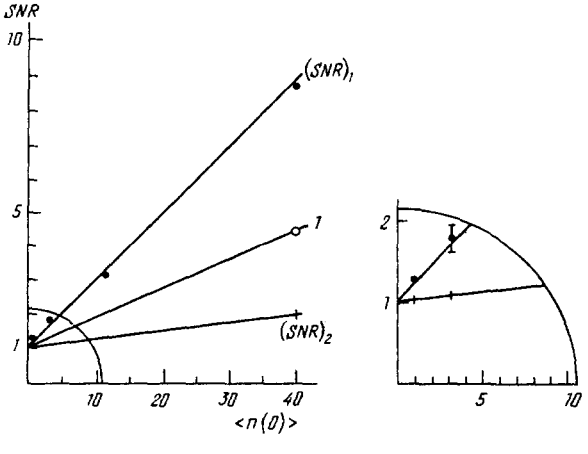

FIG. 12. Dependence of the signal-to-noise ratio SNR in channels 1 $(\mathrm{SNR})_1$ and 2 $(\mathrm{SNR})_2$ on the mean photon number per one resolution element $\langle n(0)\rangle$. The inset shows the enlarged area near the origin of coordinates.

(plane *B* 1) in the case when one of the interferometer arms is closed. The interferometer-based projection system sensitivity in this case is, naturally, by a factor of two lower than that of an ordinary scheme, since the initial signal wave is attenuated by the semi-transparent mirror 1. The signal wave and the pump wave pulses in this experiment had the same length, therefore the sensitivity of the receiving system was $\sim 5\,\hbar\omega$ per one resolution element (line *2* in Fig. 5).

If both the interferometer arms are open, the behavior of $(\mathrm{SNR})_1$ in channel 1 is observed to be practically the same as in the case without the interferometer, while in channel 2 $(\mathrm{SNR})_2$ remains close to unity. It means that the coupling of phase-conjugated beams here is coherent even when the mean photon number per resolution element in the initial signal wave approaches unity (see Fig. 12), but the total photon number in the signal beam significantly exceeds unity.

11. CONCLUSION

This paper is in the main a review of theoretical and experimental methods of research on the peculiarities of amplification and PC of weak (quantized) optical signals. The proposed semi-classical approach to describing the interaction of weak signals with matter can be applied to the analysis of diverse specific problems including, in particular, those arising in passing of beams and pulses through inhomogeneous media, beamsplitters, superregenerative amplifiers, three- and four-wave interaction in condensed and noncondensed media, etc. The above-described experimental techniques, in their turn, provide a tool not only for investigations in these problems of the special features of the spatial distribution of photon numbers averaged over the resolution elements, but also for determination of their variance and phase correlation. This holds promise for the above results to be useful in the studies of various problems of light scattering, diffraction and interference of weak signals, particularly for pulse-repetition radiation that allows for processing of massive amounts of data on the spatial distribution of light by averaging over a large number of pulses.

[1)] To form an image, it is required that $\Delta Q \gg 1$. Here and below this condition is assumed to be fulfilled.

[1] N. G. Bondarenko and V. I. Talanov, Izv. Vyssh. Uchebn. Zaved. Radiofiz. **7**, 313 (1964).
[2] G. A. Pasmanik and V. G. Sidorovich, Izv. Vyssh. Uchebn. Zaved. Radiofiz. **23**, 1217 (1980) [Radiophys. Quantum Electron. **23**, 809 (1981)].
[3] V. I. Bespalov, A. A. Betin, G. A. Pasmanik, and A. A. Shilov, Pis'ma Zh. Tek. Fiz. **5**, 242 (1979) [Sov. Tech. Phys. Lett. **5**,97 (1979)].
[4] V. I. Bespalov, A. A. Betin, A. I. Dyatlov, S. N. Kulagina, V. G. Manishin, G. A. Pasmanik, and A. A. Shilov, Zh. Eksp. Teor. Fiz. **79**, 378 (1980) [Sov. Phys. JETP **52**, 190 (1980)].
[5] N. F. Andreev, V. I. Bespalov, A. M. Kiselev, A. Z. Matveev, G. A. Pasmanik, and A. A. Shilov, Pis'ma Zh. Eksp. Teor. Fiz. **32**, 639 (1980) [JETP Lett. **32**, 635 (1980)].
[6] N. F. Andreev, V. I. Bespalov, A. M. Kiselev, G. A. Pasmanik, and A. A. Shilov, Zh. Eksp. Teor. Fiz. **82**, 1047 (1982) [Sov. Phys. JETP **55**, 612 (1982)].
[7] B. Ya. Zel'dovich, and V. V. Shkunov, Kvantovaya Elektron. (Moscow) **9**, 393 (1982) [Sov. J. Quantum Electron. **12**, 223 (1982)].
[8] O. V. Kulagin, G. A. Pasmanik, and A. A. Shilov, Izv. Akad. Nauk SSSR (Ser. Fiz.) **53**, 1619 (1989) [Bull. Acad. Sci. USSR Phys. Ser. **53**(8), 171 (1989)].
[9] V. I. Bespalov, E. L. Bubis, S. N. Kulagina, V. G. Manishin, A. Z. Matveev, G. A. Pasmanik, P. S. Razenshtein, and A. A. Shilov, Kvantovaya Elektron. (Moscow) **9**, 2367 (1982) [Sov. J. Quantum Electron. **12**, 1544 (1982)].

[10] O. V. Kulagin, G. A. Pasmanik, and A.A. Shilov, Kvantovaya Elektron. (Moscow) **16**, 1398 (1989) [Sov. J. Quantum Electron. **19**, 902 (1989)].
[11] O. V. Kulagin, G. A. Pasmanik, and A. A. Shilov, Kvantovaya Elektron. (Moscow) **17**, 355 (1990) [Sov. J. Quantum Electron. **20**, 292 (1990)].
[12] O. V. Kulagin, G. A. Pasmanik, P. B. Potlov, and A. A. Shilov, Kvantovaya Elektron. (Moscow) **17**, 1487 (1990) [Sov. J. Quantum Electron. **20**, 1395 (1990)].
[13] O. V. Kulagin, G. A. Pasmanik, P. B. Potlov, and A. A. Shilov, Kvantovaya Elektron. (Moscow) **18**, 1131 (1991) [Sov. J. Quantum Electron. **21**, (1991)].
[14] I. L. Fabelinskiĭ, *Molecular Scattering of Light*, Plenum Press, N.Y., 1968 [Russ. original, Nauka, M., 1965].
[15] V. S. Averbakh, A. I. Makarov, and A. K. Potemkin, Kvantovaya Elektron. (Moscow) **6**, 2650 (1979) [Sov. J. Quantum Electron. **9**, 1574 (1979)].
[16] V. I. Bespalov, O. V. Kulagin, A. I. Makarov, G. A. Pasmanik, A. K. Potjomkin, P. B. Potlov, A. A. Shilov, Opt. Acoust. Rev. **1**, 71 (1990).
[17] *Optical Systems with Brightness Amplifiers*, (Eds.) V. I. Bespalov and G. A. Pasmanik, Appl. Phys. Inst. Acad. Sci. USSR, Gorkiĭ, 1988 (in Russian).

English text supplied by the authors.